# Improvement of antimalarial activity of a 3-alkylpiridine alkaloid analog by replacing the pyridine ring to a thiazole-containing heterocycle: Mode of action, mutagenicity profile, and Caco-2 cell-based permeability


Daniel Silqueira Martins Guimarães, Letícia Silveira de Sousa Luz, Sara Batista do Nascimento, Lorena Rabelo Silva, Natália Rezende de Miranda Martins, Heloísa Gonçalves de Almeida, Vitória de Souza Reis, Sarah El Chamy Maluf, Alexandre Budu, Juliane Aparecida Marinho, Clarice Abramo, Adriana Karaoglanovic Carmona, Marina Goulart da Silva, Gisele Rodrigues da Silva, Victor Matheus Kemmer, Anna Paola Butera, Renato Márcio Ribeiro-Viana, Marcos Leoni Gazarini, Clébio Soares Nascimento Júnior, Luciana Guimarães, Fabio Vieira dos Santos, Whocely Victor de Castro, Gustavo Henrique Ribeiro Viana, Cristiana Ferreira Alves de Brito, Fernando de Pilla Varotti

PII: S0928-0987(19)30279-9
DOI: https://doi.org/10.1016/j.ejps.2019.105015
Article Number: 105015
Reference: PHASCI 105015

To appear in: *European Journal of Pharmaceutical Sciences*

Received date: 10 June 2019
Revised date: 11 July 2019
Accepted date: 20 July 2019

Please cite this article as: D.S.M. Guimarães, L.S. de Sousa Luz, S.B. do Nascimento, et al., Improvement of antimalarial activity of a 3-alkylpiridine alkaloid analog by replacing the pyridine ring to a thiazole-containing heterocycle: Mode of action, mutagenicity profile, and Caco-2 cell-based permeability, European Journal of Pharmaceutical Sciences, https://doi.org/10.1016/j.ejps.2019.105015

be discovered which could affect the content, and all legal disclaimers that apply to the journal pertain.

**Improvement of antimalarial activity of a 3-alkylpiridine alkaloid analog by replacing the pyridine ring to a thiazole-containing heterocycle: mode of action, mutagenicity profile, and Caco-2 cell-based permeability.**

Daniel Silqueira Martins Guimarães[a], Letícia Silveira de Sousa Luz[b], Sara Batista do Nascimento[b], Lorena Rabelo Silva[b], Natália Rezende de Miranda Martins[b], Heloísa Gonçalves de Almeida[c], Vitória de Souza Reis[c], Sarah El Chamy Maluf[d], Alexandre Budu[d], Juliane Aparecida Marinho[e], Clarice Abramo[e], Adriana Karaoglanovic Carmona[d], Marina Goulart da Silva[b], Gisele Rodrigues da Silva[f], Victor Matheus Kemmer[i], Anna Paola Butera[i], Renato Márcio Ribeiro-Viana[h], Marcos Leoni Gazarini[g], Clébio Soares Nascimento Júnior[c], Luciana Guimarães[c], Fabio Vieira dos Santos[b], Whocely Victor de Castro[b], Gustavo Henrique Ribeiro Viana[b], Cristiana Ferreira Alves de Brito[a] and Fernando de Pilla Varotti[b*]

[a]Instituto René Rachou, Fundação Oswaldo Cruz (FIOCRUZ),
1715 Augusto de Lima Avenue, Belo Horizonte, MG 30190-009, Brazil.

[b]Núcleo de Pesquisa em Química Biológica, Universidade Federal de São João Del-Rei – Campus Centro Oeste, 400 Sebastião Gonçalves Coelho Street, Divinópolis, MG, 35501-296, Brazil.

[c]Universidade Federal de São João del-Rei, Campus Dom Bosco, 74 Dom Helvécio Square, São João del Rei, MG, 36301-160, Brazil.

[d]Universidade Federal de São Paulo, Departamento de Biofísica, 669 Pedro de Toledo Street, São Paulo, SP, 04039-032, Brazil.

[e]Núcleo de Pesquisas em Parasitologia, Universidade Federal de Juiz de Fora, José Lourenço Kelmer Street, Juiz de Fora, MG 36036-900, Brazil.

[f]Universidade Federal de Ouro Preto, Departamento de Farmácia, Campus Morro do Cruzeiro, w/n, Bauxita, Ouro Preto, MG 35400-000, Brazil.

[g]Universidade Federal de São Paulo, Departamento de Biociências, 136 Silva Jardim Street, Santos, SP 11015-020, Brazil.

[h]Universidade Tecnológica Federal do Paraná, Departamento Acadêmico de Química (DAQUI) Londrina, PR, 6036-370, Brazil.

[i]Universidade Estadual de Londrina, Departamento de Química, Londrina, PR, 86057-970, Brazil
* Corresponding author

Daniel Silqueira Martins Guimarães: danielmartinsguimaraes@gmail.com

Letícia Silveira de Sousa Luz: leticia_slux@hotmail.com

Sara Batista do Nascimento: sara.bnas2@hotmail.com

Lorena Rabelo Silva: lorenarabelo6@gmail.com

Natália Rezende de Miranda Martins: naty-ande@hotmail.com
Heloísa Gonçalves de Almeida: heloisa.almeidag@outlook.com
Vitória de Souza Reis: souzareisvitoria@gmail.com
Sarah El Chamy Maluf: sarah.maluf08@gmail.com
Alexandre Budu: alexandre.budu@unifesp.br
Juliane Aparecida Marinho: jumarinho28@yahoo.com.br
Clarice Abramo: clarice.abramo@ufjf.edu.br
Adriana Karaoglanovic Carmona: ak.carmona@unifesp.br
Marina Goulart da Silva: marina@ufsj.edu.br
Gisele Rodrigues da Silva: giselersilva@ufop.edu.br
Marcos Leoni Gazarini: marcos.gazarini@unifesp.br
Clébio Soares Nascimento Júnior: clebiojunior@gmail.com
Luciana Guimarães: lucianaguimaraes8@gmail.com
Renato Márcio Ribeiro-Viana: renatoviana@utfpr.edu.br
Anna Paola Butera: paolabut@uel.br
Victor Matheus Kemmer: victorkemmer@gmail.com
Fabio Vieira dos Santos: fabiosantos@ufsj.edu.br
Whocely Victor de Castro: whocely@ufsj.edu.br
Gustavo Henrique Ribeiro Viana: viana@ufsj.edu.br
Cristiana Ferreira Alves de Brito: cristiana.brito@fiocruz.br
Fernando de Pilla Varotti: varotti@ufsj.edu.br

**Declarations of interest:** none

**Abstract**

The development of new antimalarial drugs is urgent to overcome the spread of resistance to the current treatment. Herein we synthesized the compound **3**, a hit-to-lead optimization of a thiazole based on the most promising 3-alkylpyridine marine alkaloid analog. Compound **3** was tested against *Plasmodium falciparum* and has shown to be more potent than its precursor ($IC_{50}$ values of 1.55 and 14.7 µM, respectively), with higher selectivity index (74.7) for noncancerous human cell line. This compound was not mutagenic and showed genotoxicity only at concentrations four-fold higher than its $IC_{50}$. Compound **3** was tested *in vivo* against *Plasmodium berghei* NK65 strain and inhibited the development of parasite at 50 mg/kg. *In silico* and UV-vis approaches determined that compound **3** acts impairing hemozoin crystallization and confocal microscopy experiments corroborate these findings as the compound was capable of diminishing food vacuole acidity. The assay of uptake using human intestinal Caco-2 cell line showed that compound **3** is absorbed similarly to chloroquine, a standard antimalarial agent. Therefore, we present here compound **3** as a potent new lead antimalarial compound.

**Keywords**

*Plasmodium falciparum*, 3-alkylpyridine marine alkaloid analogs, antiplasmodial activity, thiazole, malaria, ferriprotoporphyrin-IX**.**

**Abbreviations**

3-APA: 3-alkylpyridine marine alkaloid

ACTs: Artemisinin-based Combination Therapies

ADMET: absorption, distribution, metabolism, excretion and toxicity

AO: Acridine Orange

AS: Artesunate

CBMN: Cytokinesis-Block Micronucleus

CQ: Chloroquine

DAPI: 4',6-diamidino-2-phenylindole

DFT: Density Functional Theory

DMSO: Dimethyl sulfoxide

ELISA: Enzyme-Linked Immunosorbent Assay

FBS: Fetal Bovine Serum

Fe(III)PPIX: Ferriprotoporphyrin-IX
HBSS:Hanks' Balanced Salt solution
HPLC: High-performance liquid chromatography
HRMS: High Resolution Mass Spectrometry
HRPII: Histidine-Rich Protein II
$IC_{50}$: Inhibitory concentration 50%
IR: Infrared
MMS: Methyl methanesulfonate
MQ: Mefloquine
MTT: 3-(4,5-dimethylthiazol-2-yl)-2,5-diphenyltetrazolium bromide
NDI: Nuclear Division Index
NMR: Nuclear magnetic resonance
OD: Optical Density
RBC: Red Blood Cell
SD: Standard Deviation
SI: Selectivity Index
PBS: Phosphate Buffered Saline
PMSF: phenylmethylsulfonyl fluoride
TM: Transport Medium
TMS: tetramethylsilane

## 1. Introduction

More than 3 billion people live in areas with potential risk of malaria transmission, the most important mosquito-borne infectious disease (Ferrao et al., 2018; Walker et al., 2018). The World Health Organization estimated that, in 2017 occurred throughout the world 219 million malaria cases resulting in approximately 435,000 deaths. Five species of *Plasmodium* commonly infect humans, *P. falciparum*, *P. vivax*, *P. ovale*, *P. malariae* and *P. knowlesi.* Among these species *P. falciparum* is the most virulent being responsible for more than 90% of the cases and deaths (WHO, 2018). In the absence of an efficient vaccine, malaria treatment relies on Artemisinin-based Combination Therapies (ACTs) (Martin et al., 2018; Nsanzabana, 2019). However, the

burden and widespread resistance of parasites to the current antimalarial drugs impair the elimination of the disease (Martin et al., 2018). In this scenario, the need for the development of novel effective drugs against resistant *P. falciparum* strains is of paramount importance (Mishra et al., 2017).

The determination of new active antimalarial compounds is not always associated with the description of their potential targets (Lobo et al., 2018; Thakur et al., 2018). The lack of knowledge about the mode of action of a new antimalarial compound can negatively affect preclinical tests and hinder the employment of rational strategies to improve compound potency and selectivity (Skinner-Adams et al., 2016).

Taking into account all these requirements, our research group has designed and synthesized new 3-alkylpyridine marine alkaloid (3-APA) analogs with antiplasmodial activity (Barbosa et al., 2017; Hilário et al., 2011; Ribeiro-Viana et al., 2016). Based on rational approaches, combining *in silico* and biophysical data, we have demonstrated that these 3-APA analogs were able to form stable complexes with ferriprotoporphyrin-IX (Barbosa et al., 2017; Ribeiro-Viana et al., 2016).

The inhibition of hemozoin formation in malarial parasites remains an attractive target for the development of new antimalarial drugs (Ashley and Phyo, 2018). During the erythrocytic stage, malaria parasites use amino acids resulting from the breakdown of hemoglobin (Hb) present in red blood cells for its growth; however, the free heme (ferriprotoporphyrin-IX) generated in this process is highly toxic to the parasite. Therefore, heme polymerization is a detoxification strategy adopted by the malaria protozoan to convert toxic heme into a non-toxic polymerized crystal called hemozoin (Egan, 2008). This pathway is vital for parasite survival and the inhibition of heme polymerization results in the death of the protozoan (Singh et al., 2014).

In the specific context of malaria, heterocycles play a critical role in their antiplasmodial activity according to a recent literature review (Kalaria et al., 2018). Many heterocyclic compounds have high antimalarial activity and better ADMET properties in pre-clinical studies. Furthermore, we recently reported that the pyridine ring is critical to the antiplasmodial activity of 3-APA analogs (Barbosa et al., 2017; Ribeiro-Viana et al., 2016). However, the pyridine heterocycle is known to be toxic to living organisms (Lodha et al., 2008; Mudliar et al., 2008; Padoley et al., 2006).

Due to practical, patient compliance, cost-effectiveness, and safety reasons antimalarial drugs are preferably developed as solid oral dosage forms. It means that the drug compound must fulfill physicochemical requirements to achieve adequate bioavailability, which is driven by dissolution, permeability, solubility, absorption, metabolism, and excretion (Zhu et al., 2017).

However, many potential new antimalarial candidates described in drug discovery process find a pitfall in such properties impairing or simply preventing the drug candidate to be administered orally (Mishra et al., 2017). To overcome these limitations, this work describes the optimization of a previously synthesized 3-APA which has its antimalarial activity enhanced by replacing the pyridine ring to a thiazole heterocycle providing a rational scaffold for new antimalarials candidates.

## 2. Material and Methods

### 2.1. *Chemistry*

Reagents and solvents were purchased as reagent grade from Sigma-Aldrich and used without further purification. NMR spectra were recorded using Bruker Avance DRX-200. Chemical shifts are reported as $\delta$ (ppm) downfield from tetramethylsilane (TMS),

and the *J* values are reported in Hz. IR spectra were recorded using a Shimadzu IRAffinity-1 Fourier transform spectrometer. High-resolution mass spectrometry (HRMS) was recorded using an ESI micrOTOF-QII Bruker mass spectrometer. Column chromatography was performed with silica gel 60, 70–230 mesh (Merck, Darmstadt, Germany). Interaction studies were carried out in a UV-vis spectrophotometer (Shimadzu, Model UV-2600) equipped with a thermoregulator (Peltier, Model S-1700) at 25 °C, using 1 cm path cuvettes.

## 2.2. *Synthetic routes*

### 2.2.1. *Synthesis of 10-((4,5-dihydrothiazol-2-yl)thio)decan-1-ol 3*

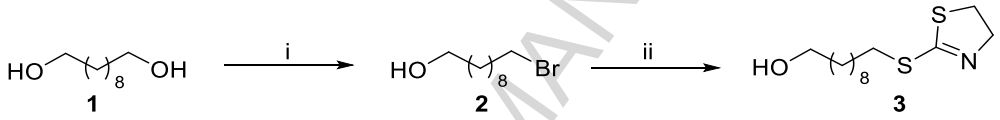


Reagents, conditions, and yields: (i) HBr, toluene, reflux, 16h, 74%; (ii) 2-thiazoline-2-thiol, KOH, ethanol/water (3:2), MW, 100W, 25°C→60°C, 15min, 97%.

Scheme 1: Synthetic route to 10-(4,5-dihydrothiazol-2-yl)thio)decan-1-ol 3) **(1)**.

### 2.2.2. *Synthesis of 10-bromo-decan-1-ol 2*

Hydrobromic acid (1.2 mL 48% aqueous solution, 9.5 mmol) was added to a suspension of 1,10-decanediol **1** (1.5 g, 8.6 mmol) in 30 mL of toluene in a round-bottomed flask equipped with a Dean-Stark trap and a cooler. The mixture was refluxed for 16h. After cooling, the solvent was removed under reduced pressure. The residue obtained was chromatographed on silica gel using hexane/ethyl acetate (8:2) to yield the pure compound **2**.

Yield 74%; yellow oily product: IR (KBr): $\bar{\nu}$ = 3325, 2925, 2850, 1450, 1250, 1050, 700, 625, 550 $cm^{-1}$. $^1H$ NMR (200 MHz, $CDCl_3$): $\delta$ 1.20-1.40 (m, 12H), 1.45-1.60

(m, 2H), 1.84 (qn, *J*= 6.8Hz, 2H), 3.39 (t, *J*= 6.8Hz, 2H), 3.62 (t, *J*= 6.4Hz, 2H) ppm. $^{13}$C NMR (50 MHz, $CDCl_3$) $\delta$: 25.67, 28.11, 28.69, 29, 32, 29.42, 32.73, 32.77, 33.98, 62.99 ppm.

### 2.2.3. *Synthesis of 10-(4,5-dihydrothiazol-2-yl)thio)decan-1-ol) 3*

A 25 mL round-bottomed flask containing a mixture of 10-bromedecan-1-ol (0.42 mmol), 2-thiazoline-2-thiol (0.46 mmol) and potassium hydroxide (0.46 mmol) in 10 mL of ethanol/water (3:2) was placed in a CEM Discover microwave oven (open vessel mode). Microwave irradiation of 100 W was used, and the temperature was ramped from 25 °C to 60 °C. Once 60 °C was reached, in around 3 min, the reaction mixture was held at this temperature for 15 min, under stirring. All temperatures were measured externally by an IR sensor. The reaction mixture was cooled to room temperature and then extracted with ethyl acetate (3×15 mL). The organic extracts were combined and dried ($Na_2SO_4$), and the solvents were removed under reduced pressure. The residue obtained was chromatographed on silica gel using hexane/ethyl acetate (6:4) to yield the pure compound **3**.

Yield 97%; yellow oily product: $^1$H NMR (200 MHz, $CDCl_3$): $\delta$ 1.15-1.4 (m, 12H), 1.4-1.6 (m, 2H), 1.6-1.7 (m, 2H), 3.08 (t, *J*=7.2Hz, 2H), 3.36 (t, *J* = 7.4Hz, 2H), 3.65 (t, *J* =5.2Hz, 2H), 4.20 (t, *J* =7.6 Hz, 2H) ppm. $^{13}$C NMR (50 MHz, CDCl3): $\delta$ 25.63, 28.60, 28.94, 29.13, 29.25, 29.36, 32.66, 32.72, 35.16, 62.79, 64.21, 166.16 ppm. HRMS (*m/z*): $[M + H]^+$ = 276.1451 (theoretical 276.1378).

## 2.3. *In silico analysis*

Density Functional Theory (DFT) calculations were performed in order to obtain structures and binding energies for the process involving two compounds, the compound **3** and their active site, the ferriprotoporphyrin-IX heme group [Fe(III)PPIX],

in 1:1 molar ratio. In the present work, we have used the same theoretical methodology (UB3LYP/GEN) as described in our recent papers (Barbosa et al., 2017, 2018; Ribeiro-Viana et al., 2016). The UB3LYP binding energy (ΔE) related to this linking process was obtained. All theoretical calculations were performed using the Gaussian 09 quantum mechanical package.

## 2.4. Heme Binding Experiments

### 2.4.1. DMSO/HEPES Buffer (40% v/v)

1.1906g of HEPES was dissolved in 5 mL of distilled water. This solution was transferred to a 250 mL volumetric flask containing 100 mL of DMSO. The remaining volume was filled with distilled water up to 250 mL and the pH was adjusted to 7.4.

### 2.4.2. Hematin Stock solution (0.0026 mol/L)

17.2 mg of hemin (Sigma-Aldrich) was transferred to a 10 ml volumetric flask and filled with DMSO/HEPES buffer (pH 7.4).

### 2.4.3. Hematin analysis solution (5 µmol/L)

48 µL of hematin stock solution was transferred to a 25 mL volumetric flask and filled with DMSO/HEPES buffer (pH 7.4). This solution was prepared daily.

### 2.4.4. Compound 3 stock solution (68.97 mmol/L)

15.2 mg of compound **3** was weighted in an eppendorf and dissolved in 800 uL of DMSO.

### 2.4.5. Compound 3 analysis solution (8.10 mmol/L)

94 µL of compound **3** stock solution was mixed with 706 µL of hematin analysis solution (SAhm) in an eppendorf.

### 2.4.6. Compound 3-hematin Titration experiment

Two cuvettes were used to perform the titration assay, blank and test. Blank cuvette was filled with 2.5 mL of DMSO/HEPES buffer and test curvet with 2.5 mL of hematin analysis solution. To the test solution were added incremental volumes of compound **3** analysis solution, under magnetic stirring. After each hematin solution addition, one minute was holding on before the scanning in the UV-Vis range (200 nm to 500 nm) was performed. After each reading, the ƛmax was recorded as 401 nm. All the experiments were performed in triplicate. Curve fitting was performed using GraphPad Prism 5.01 software.

### 2.5. *Biological evaluation*

#### 2.5.1. *In vitro schizonticidal activity against P. falciparum*

The *P. falciparum* chloroquine-resistant (W2) strain was maintained in continuous culture using human red blood cells in RPMI 1640 medium supplemented with human plasma. Human red blood cells and human plasma were provided by the Foundation of Hemotherapy and Hematology of Minas Gerais (Fundação Hemominas). The parasites were synchronized using sorbitol treatment (Lambros and Vanderberg, 1979) and the parasitemias were microscopically evaluated with Giemsa-stained blood smears. The antimalarial activity was determined using an anti-HRPII assay (Noedl et al., 2002). Infected red blood cells were incubated on a 96-well plate at 0.05 % parasitemia and 1.5% hematocrit. Different concentrations of the drugs were added in triplicate and twelve drug-free wells were used as controls (six frozen after 24 h as the HRPII background). After incubation (72 h), the plate was frozen, thawed twice and an ELISA using anti-HRPII antibodies was performed. The results were expressed as the mean of the half-maximal inhibitory dose ($IC_{50}$) of three assays with different drug concentrations performed in triplicate, compared with drug-free controls. Curve fitting

was performed using Origin Pro 8.0 software (Origin Lab. Corporation, Northampton, MA, USA). Chloroquine (Sigma-Aldrich) was used as antimalarial standard.

### 2.5.2. *In vitro* cytotoxicity evaluation

The noncancerous human lung fibroblast cell line WI-26-VA4 (ATCC CCL-95.1) was used to assess the cell viability after each chemical treatment employing the MTT colorimetric assay (Carmichael et al., 1987). Briefly, $1 \times 10^6$ cells were seeded on 96-well plates in RPMI 1640 medium supplemented with fetal bovine serum (FBS) and penicillin-streptomycin antibiotics. Then, plates were incubated overnight at 37 °C, 5% $CO_2$, followed by the treatment with each compound solubilized in DMSO. Negative control groups were constituted of cells without treatment. Five serial dilutions (from 100 to 0.01 $\mu g.mL^{-1}$) were made from a stock solution (10 $mg.mL^{-1}$) using RPMI supplemented with 1% FBS. After 48 h of incubation, cell viability was evaluated by discarding the medium and adding 100 µL of MTT 0.05 %, followed by 3 h of incubation. Then, the supernatant was discharged, and the insoluble formazan product was dissolved in DMSO. The optical density (OD) was measured using a microplate spectrophotometer at 570 nm. The OD in untreated control cells was defined as 100 % cell viability. All assays were performed in triplicate. The selectivity index (SI) was calculated as SI = $IC_{50}$ WI-26-VA4 / $IC_{50}$ *P. falciparum*.

### 2.5.3. *Alkaline Comet Assay*

The alkaline comet assay (single-cell gel electrophoresis assay) was performed according to Olive and Banáth (2006) with adaptations. Briefly, RKO-AS45-1 (ATCC CRL-2579) cells were seeded in 24-well plates ($2 \times 10^5$ cells/well) in complete medium and the treatments were performed after 24 h. The cells were exposed to different concentrations of the compound **3** (3.6 µM, 7.25 µM, and 14.55 µM) for 3 h in culture

medium without serum. The cells of the positive control group were treated with methyl methanesulfonate (MMS - 120 µM) (Sigma-Aldrich) and the negative control group was treated with PBS (phosphate buffered saline). The quantification of chromosomal damages was achieved by visual scoring, based on the comets classification from 0 (no damage) to 4 (maximum damage) (Collins, 2004). For each treatment, 100 comets were analyzed and the calculation of the scores was performed employing the equation Score = 0(C0) + 1(C1) + 2(C2) + 3(C3) + 4(C4), where C0–C4 are the numbers of comets in each classification of damage. Three independent experiments were performed and a mean of the scores obtained was calculated for each treatment. In the statistical analysis, ANOVA (Analysis of Variance) was performed followed by the Tukey-Kramer multiple comparisons post-test with a significance level of 0.05 (de Oliveira et al., 2017).

#### 2.5.4. *Cytokinesis-Block Micronucleus (CBMN) Assay*

To assess the potential of compound **3** to induce chromosomal mutations *in vitro*, the cytokinesis-block micronucleus (CBMN) assay was performed in the RKO-AS45-1 (ATCC CRL-2579) human cell line, with and without metabolic activation (S9 fraction). The procedures were carried out as described by Fenech (2007) with adaptations. Briefly, 2.5 x $10^5$ cells/well were seeded in 24-well plates in complete medium and the treatments were performed for 24 h. MMS (400 µM) was used as positive control and the negative control group received culture medium without serum as treatment. Compound **3**, diluted in culture medium without serum, were evaluated in three different concentrations (3.6 µM, 7.25 µM, and 14.55 µM) and three independent experiments were conducted under these conditions, with or without metabolic activation. After 3 h of treatment, cells were washed and fresh complete medium containing cytochalasin-B (Sigma-Aldrich) (3.0 µg.mL$^{-1}$) was added for 24 h. Next,

cells were processed for the slides confection. Slides were stained with DAPI (4',6-diamidino-2-phenylindole – 1 μg.mL$^{-1}$) (Sigma-Aldrich) diluted in PBS for cytogenetic analysis under a fluorescent microscope (Zeiss, Axioscope A1) with an excitation filter of 365 nm and a barrier filter of 445/450 nm. In a blind test, one thousand binucleated cells were analyzed for each treatment and cells containing 1–3 micronuclei were scored (Gomes et al., 2011), following the criteria for the identification of micronuclei (MNs) described by Titenko-Holland et al., 1997. For statistical analysis, ANOVA was performed followed by the Tukey's Multiple Comparison post-test with a significance level of 0.05. The influence of compound **3** on cell proliferation was assessed by calculating the Nuclear Division Index (NDI) in the same slides prepared for the CBMN assay. Three hundred cells with well-preserved cytoplasm were counted using fluorescence microscopy, as described above. The NDI was calculated according to Eastmond and Tucker (1989) and Fenech (2007), using the equation NDI = (M1 + 2(M2) + 3(M3) + 4(M4))/N, where M1–M4 are the numbers of cells with 1, 2, 3 and 4 nuclei, respectively, and N is the total number of analyzed cells.

**2.5.5.*Live Cell Imaging***

Synchronous trophozoites of *P. falciparum* (W2 strain) were marked with the lysosomotropic probe acridine orange (AO) (Sigma-Aldrich) ( as described by Bennett and colleagues (2004) with modifications. Briefly, the culture with 10 % parasitemia was centrifuged for 5 min at 9,000 *x g* and resuspended in RPMI without phenol red. The RBC number was determined using a Neubauer chamber and it was adjusted to $1\times10^7$ RBC.mL$^{-1}$ of RPMI medium supplemented with 5 μM AO. The sample was incubated for 40 min at 37 ºC. After that, cells were washed three times and 500 μL transferred to a four-chamber petri dish (Cell view glass - Greiner Bio-one). Fluorescence images was acquired using a multiphoton scanning microscope (LSM 780

Zeiss, Germany) with parameters: 488 nm exciting wavelength and collecting fluorescence emission between 560-615 nm. AO fluorescence localization and intensity were measured before and after a 3 minute-treatment with compound **3** and CQ. Experiments were performed in triplicate and each parasite cell was analyzed independently.

### 2.5.6. *In vivo evaluation of the antimalarial activity*

For *in vivo* assays, female Swiss mice, 4 to 6 weeks of age provided by the Center for Reproductive Biology of Universidade Federal de Juiz de Fora (Ethics committee approval process nº 043/2016) were kept in micro isolated cages and inside ventilated shelves (ALESCO), maintained at controlled temperature (22 ± 2 ºC), 60-90 % humidity under a 12 h light/dark cycle with free access to food and water.

The suppressive test was performed according to Peters (1965), with modifications. The animals were randomly divided, and after weighing, the inoculum of 0.2 mL solution was adjusted to $5\times10^6$ infected erythrocytes/mL *P. berghei* NK65 in RPMI medium (Cultilab) supplemented with 10 % fetal bovine serum (Sigma-Aldrich). After 4 h of the infection, mice were treated by gavage with 0.1 mL of the compound **3** and the association of Artesunate (Sigma-Aldrich) (5 mg/kg) and Mefloquine (Sigma-Aldrich) (10 mg/kg) diluted in 5 % dimethyl sulfoxide (DMSO) and filtered water for 4 days. The compounds were tested at doses of 50, 20 and 10 mg/kg. The parasitaemia was determined by Giemsa-stained smears with blood collected from caudal vein at the $5^{th}$, $7^{th}$, $9^{th}$ and $12^{th}$-day post-infection (d.p.i). Mice survival was evaluated for 30 days. Inhibition of parasite multiplication (IPM) was calculated by the difference between the mean of the parasitaemia of the group not treated by the mean of the tested group, divided by the mean of that from the untreated group, expressed as a percentage (Andrade-Neto et al., 2003).

**2.5.7.*Caco-2 cell culture and in vitro uptake***

Human intestinal Caco-2 cells provided by American Type Culture Collection ATCC (Rockville, MD, USA) were cultured for 21 days with Dulbecco´s Modified Eagle Medium (DMEM) high glucose supplemented with 10 % of fetal bovine serum, 1 % of nonessential aminoacids, 100 $U.mL^{-1}$ penicillin G, 100 $mg.mL^{-1}$ streptomycin, 1.25 $mg.mL^{-1}$ amphotericin B, and 10 mM sodium pyruvate in tissue culture test plate. All of them from Sigma Chemical Company (St. Louis, MO). The atmosphere was kept with 90–95 % relative humidity, 37 °C, 5 % $CO_2$ and 9 5% air.

In the experiment day, DMEM was removed and the cells were incubated with compound **3** (15, 30 and 60 min.) and chloroquine for 60 min. After incubation the solutions were removed, cells were washed three times with ice-cold transport medium (TM) consisted of Hank´s balanced salt solution pH 7.4 (0-4 $^{o}$C). The cells were lysed with 400 µL of NaOH (1M) and sonicated for 2 minutes. The suspension was neutralized with HCl (1M), sonicated for additional 2 minutes, and centrifuged at 22,000 x g for 10 min at 15 °C. The supernatant (400 µL) was transferred for vials and 75 µL were injected in the HPLC for quantification. The pellets were sonicated in an Unique ® DES500 ultrasonic cell disruptor (Indaiatuba, Brazil) and the protein content was measured by the Bradford method (Bradford, 1976). Sonication was conducted under ice bath using three cycles of 30 sec. on at 30% of potency and 10 sec. off.

Stock solutions of compound **3** and chloroquine at 10,000 µM were prepared in ethanol and transport medium (TM), respectively, whereas, the work solutions (100 µM) of both compounds were prepared in TM.

Compound **3** and chloroquine detection were performed by high pressure liquid chromatograph. Briefly, separation of the compounds was achieved using a 150 x 4.00 mm column packed with 5 µm ODS (octadecylsilane) particles (NST®, São Carlos,

Brasil) at 40 °C. For the compound **3** analysis the mobile phase consisted of acidified water (pH 3.2) and methanol (25:75). The flow rate was 1.2 mL/min and the detection occurred at 232 nm. The chloroquine was detected at 245 nm using as mobile phase acetonitrile and aqueous solution (pH 3.4) containing 1-heptanesulfonic acid (20 mM) and diethylamine (0.07%) (30:70, v/v) at a flow rate of 1.0 mL/min, according to the method described by Yonemitsu (2005). In both cases the pH of the aqueous phase was previously adjusted with phosphoric acid.

The uptake studies were conducted in triplicate and the results (ng/mg of protein) expressed as mean ± sd. Compound **3** and chloroquine intracellular concentration were compared using One-Way ANOVA followed by the test of Tukey for multi-comparison. A value of $p < 0.05$ was considered significant.

## 3. Results and Discussion

### 3.1. *Heterocycle change*

In our previous work (Barbosa et al., 2017) we reported the synthesis of a series of 3-APA analogs and the identification of a hit compound **4** among them with the lowest $IC_{50}$ values of the series, and the highest SI (Figure 1).

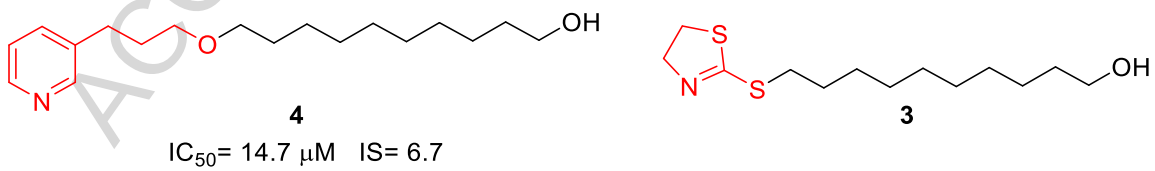


**Figure 1**. Previously synthesized 3-APA analog **4** and the optimized compound **3** with the moiety derived from 3-pyridinopropanol and the new thiazole ring. The pyridine and thiazole rings are highlighted in red.

Therefore, compound **4** was selected as a starting point to lead optimization. The thiazole core was selected for pyridine replacement, supported by successfully reported cases of new potential synthetic antimalarials compounds with enhanced activity (Kumawat, 2017; Sharma et al., 2019).

A recent report described the antimalarial activity of several compounds containing imidazopyridine heterocycle with low toxicity (Baker et al., 2017). A subsequent study demonstrated that the substitution of imidazopyridine heterocycle by a thiazole core resulted in a potent scaffold with nanomolar range activity against *P. falciparum* intraerythrocytic stages (Penzo et al., 2019).

Herein, we have focused our development on the removal of the potentially toxic pyridine ring represented by the commercially 3-pyridinopropanol moiety used to synthesize the 3-APA analog and change it to a thiazole heterocycle (Figure 1).

However, this alteration on the structure of the compound **4** could affect the molecular recognition of heme group. To examine this possibility, we carried out *in silico* and UV-vis analysis.

### 3.2. *In silico Thiazoline-heme binding*

The ferriprotoporphyrin-IX [Fe(III)PPIX] interaction with compound **3** has been investigated. The optimized geometry for the complex, in which the nitrogen atom of thiazole ring binds to Fe(III) ion, is depicted in Figure 2. The calculated UB3LYP/GEN binding energy is -12.5 kcal.mol$^{-1}$. It can be observed that the formation of 1:1 compound **3** complex with Fe(III)PPIX is energetically favored, as also observed for pyridine ring in our previous works (Barbosa et al., 2017, 2018; Ribeiro-Viana et al., 2016). In both cases the nitrogen atom of heterocyclic ring is the responsible for the binding. Finally, the DFT (UB3LYP/GEN) theoretical analysis indicated that, based on

the energetics of binding process, the heme group can be considered a target for the compound **3**.

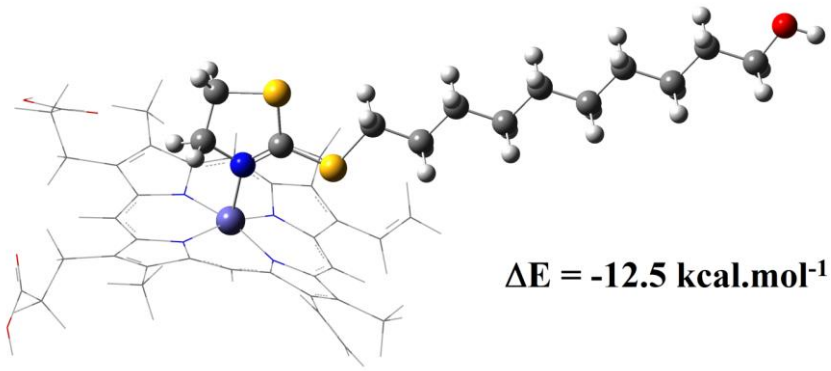


**Figure 2.** UB3LYP optimized geometry for the compound **3-[Fe(III)PPIX]** complex in a 1:1 molar ratio.

### 3.3. *Hematin binding studies*

Hematin binding studies using UV-vis titration were performed to identify the behavior of compound **3** in the presence of hematin and confirm it as a target. This experiment provides an important qualitative data of the formation of supramolecular complex. The complex formation is observed by the pattern of the isotherm formed after the data analysis. The data collected in this work, exhibited a different pattern of curve from the others compounds synthesized by our group (Figure 3).

The absorbances during the addition of compound **3** showed three different moments: a small decrease in the beginning, followed by increase of the observed absorbance and finally a trend of a plateau. Our previous synthesized molecules showed different isotherm pattern (Barbosa et al., 2017, 2018; Ribeiro-Viana et al., 2016). It was observed a decrease in absorbance values as the concentrations of added ligand were increased, indicating that those complexes have lower molar absorption than

hematin. In this particular case, a plateau is not formed soon after the decrease of the absorbances, but after an increase of it. This kind of pattern suggests a different mode of interaction of this molecule with hematin. Simulation of isotherm in different scenarios via Supramolecular website (Thordarson, 2011; Hibbert and Thordarson, 2016) showed a ternary complex in which the first ligand-host complexation had lower molar absorptivity, in comparison to free hematin. In addition, it was observed a second ligand binding to the complex with higher molar absorptivity. Therefore, these data suggest that the replacement of pyridine ring by thiazoline group in compound **3** kept the hematin as a target with lower affinity in solution, and changed the binding mode.

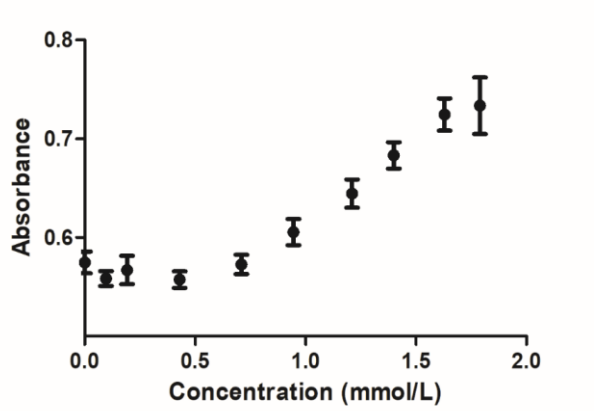


**Figure 3.** Titration of heme (5 µmol/L) with increasing concentration of compound **3** (0−1,9 mmol/L) at A401 nm.

### 3.4. *In vitro antiplasmodial activity*

The compound **3** was tested against *P. falciparum* W2 strain and showed an $IC_{50}$ value of 1.55 µM (Table 1), which is more than 9-fold lower than the $IC_{50}$ of its precursor **4** (14.7 µM) (Barbosa et al., 2017). The cytotoxicity evaluation showed that, both the precursor and the compound **3,** exhibited similar $IC_{50}$ against human WI26VA-4 cell line (99.1 and 115.8 µM, respectively). The choice of chemical starting points for the development of new potential antimalarial candidates is crucial for success of

clinical studies (Mishra et al., 2017). In this sense, a set of specific criteria for defining hits and leading compounds were proposed in the development of new drug candidate against malaria. (Katsuno et al., 2015). For *in vitro* assays, compound **3** exhibits potency around 1–2 μM and the SI is greater than 10-fold against a human cell line.

To examine the safety of compound **3** we performed genetic toxicological studies.

### 3.5. *Genotoxicity evaluation*

Cytokinesis-Block Micronucleus (CBMN) Assay showed that compound **3** did not induce the formation of micronuclei compared to the control (PBS). This assay is required for drug development to determine mutagenicity by detecting both clastogenic and aneugenic agents (Kirsch-Volders et al., 2014). The Alkaline Comet assay, that detects DNA breaks, was also performed and three concentrations were evaluated. Compound **3** was only genotoxic at 7.25 μM and 14.55 μM but not at 3.6 μM. This result indicates that even though at some point the compound induces DNA strand breaks, the concentration required is more than 4.5 times higher than the $IC_{50}$ for *P. falciparum*. Nevertheless, these primary DNA damages were not fixed as mutations as verified in CBMN assay. In studies performed with and without metabolic activation with the S9 fraction, the exposition to compound **3** did not induce a significant increase in the frequency of micronucleated cells (Table 1, Figure 4).

The evaluation of the genotoxicity of compounds with pharmacological potential is an important step in the pathway of a drug registration process, once gene mutations and chromosomal aberrations are related with degenerative diseases and heritable disorders (Ji et al., 2017). In this way, results presented herein are very promising in the toxicological assessment of this drug prototype once the assays performed showed that DNA damages were induced only in concentrations much higher than the $IC_{50}$ obtained in *P. falciparum*. In addition to data collected in human cell line, the cells were able to

repair the damage, preventing the fixation of mutations. It is important to highlight that new antimalarial medicines must be safe in specific patient groups, such as: i) pregnant women, ii) youngest children, iii) and patients with co-morbidities, like HIV (Burrows et al., 2017). Moreover, a previous study of our study group (Gonçalves et al., 2014) showed that the compound **4** was mutagenic in the CBMN assay carried out with the same cell line used in present work.

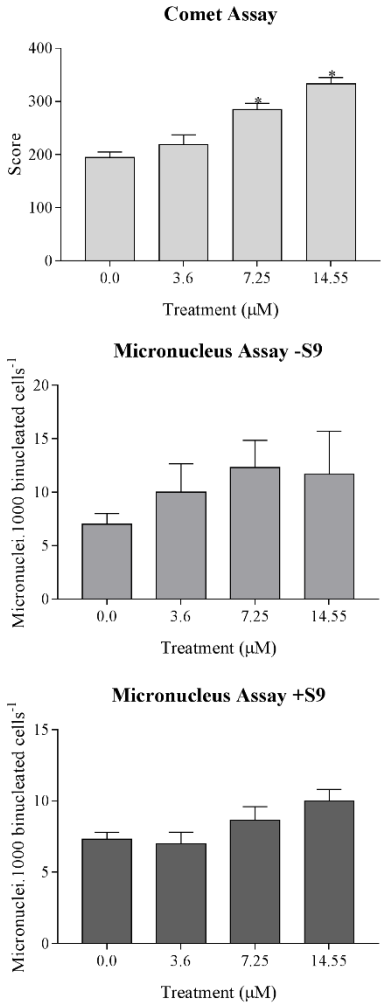


**Figure 4.** Score values obtained for Compound 3 in Alkaline Comet Assay and frequency of binuclated cells with micronuclei observed in CBMN assay, with (+S9) and without (-S9) metabolic activation *in vitro*. * Statistically significant ($p<0.05$) when compared to negative control (0 µM).

**Table 1.** Antiplasmodial, cytotoxicity and mutagenicity of compound **3** compared to Chloroquine

| | $IC_{50}$ (µM ± S.D.) | | SI | Comet (*µM) | CBMN +S9/-S9 |
|---|---|---|---|---|---|
| | *P. falciparum* | WI26VA-4 | | RKOAS45-1 | |
| **3** | 1.55 ± 0.27 | 115.8 ± 5.7 | 74.7 | 7.25 | NM/NM |
| Chloroquine | 0.38 ± 0.09 | >100 | >250 | NT | NT |

S.D. = Standard Deviation; SI = Selectivity Index; NM = not mutagenic for every concentration tested; NT = not tested; *Lowest concentration in which genotoxicity was detected

### 3.6. *Analysis of food vacuole pH alterations*

After the *in vitro* analysis was performed, and the *in silico* model revealing insigths of compound **3** mode of action, our goal has been to probe infected red blood cells with AO to determine food vacuole as a potential intracellular target to the compound **3**. Food vacuole is the organelle in Plasmodium responsible for hemoglobin digestion and highly dependent of internal pH (Singh et al., 2014). The treatment with compound **3** and CQ occurred for 3 min. Both compounds were tested at their $IC_{50}$ (1.55 µM for **3** and 0.38 µM for CQ). Figure 5 shows the decrease in fluorescence intensity after treatment with both compounds.

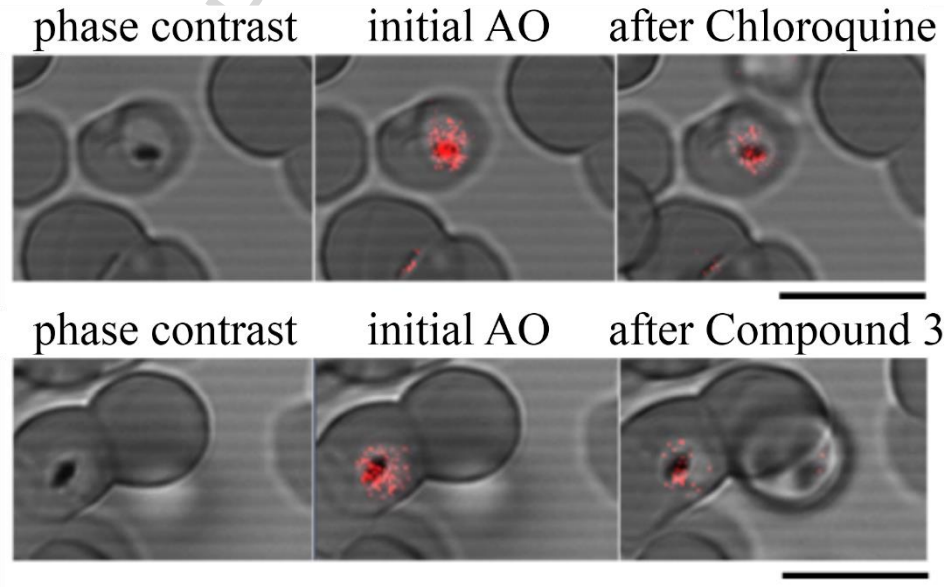

**Figure 5.** Confocal imaging of *P. falciparum* W2 loaded with Acridine Orange before and after the addition of Chloroquine (0.38 µM) and compound **3** (1.55 µM). Food vacuole alkalinization was evaluated for 180 seconds (3min) after addition of the compounds. Scale bar 10µm.

The drop of AO fluorescence in food vacuole selected area is observed after the addition of compound **3** in a graph of fluorescence intensity *versus* time (Figure 6).

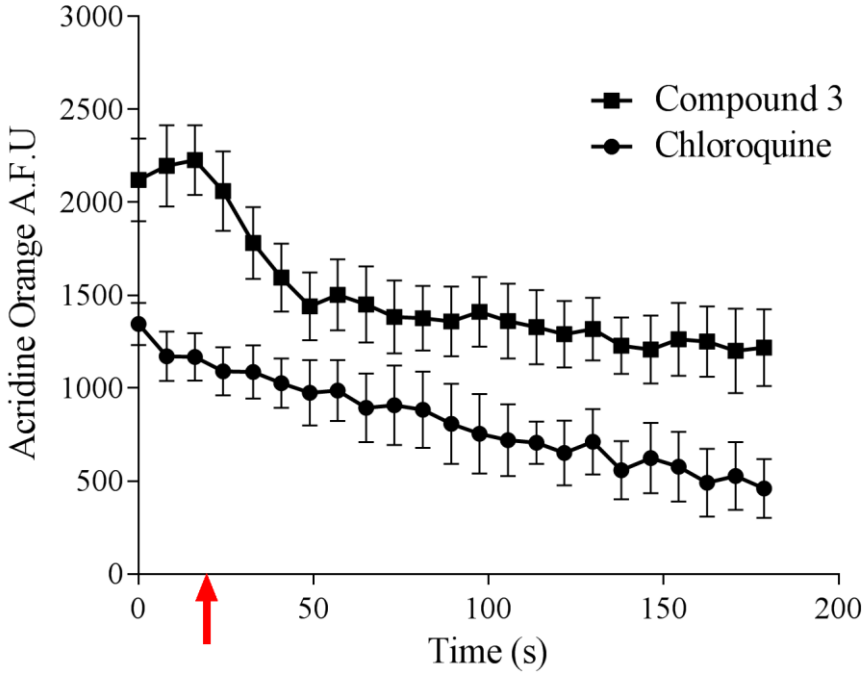


**Figure 6.** Fluorescence measurement of acridine orange in food vacuole selected areas by confocal microscopy. Chloroquine (CQ) and compound **3** were added at the beginning of the measurement and AO fluorescence was evaluated for 180 seconds. Fluorescence intensities (arbitrary fluorescence units - AFU) represent at least three different cell preparations. The red arrow indicates the moment of CQ and compound **3** addition.

Acridine orange accumulates inside acid organelles, such as lysosome and the parasite's food vacuole and it emits red fluorescence (>560 nm) and little green fluorescence (500-530 nm) when inside nucleus and cytoplasm (El Chamy Maluf et al., 2016). Confocal analysis showed that the compound **3** interferes in the proton homeostasis ($H^+$), since the fluorescence of the digestive vacuole decreased with the treatment, making this organelle less acidic. Therefore, the differences between the initial fluorescence (f0) and final fluorescence (f1), using Student's t-test, were

evaluated to compare the mean fluorescence difference between the two treatments. No statistical difference between the treatments was observed.

### 3.7. *In vivo antimalarial assays*

Considering that the $IC_{50}$ value obtained to *P. falciparum* is now under 2 µM, as suggested by Katsuno (2015), we decided to proceed to test the compound **3** for its *in vivo* antimalarial activity. Three treatment doses were tested (50, 20 and 10 mg/kg) during four days on previously *P. berghei* NK65 infected swiss mice. At the fifth day of the experiment, 50 mg/kg of compound **3** reduced almost 65 % of the parasitaemia compared to the control group. However, the reduction did not persist on the following days. The doses of 10 and 2 0mg/kg reduced 19.2 and 26.5 % of the parasitaemia on the first day post-treatment, respectively, however, this reduction disappeared at the ninth day and beyond. The drugs used as standard antimalarials were artesunate and mefloquine, with doses of 5 and 10 mg/kg, respectively. This treatment reduced at least 90 % of the parasitemia at the 4 days evaluated (Table 2, Figure 7).

**Table 2.** Parasitemia and percentage reduction at different days post inoculation on swiss female mice

| Compound | Dose (mg/kg) | Parasitaemia ± SD (% Reduction) at day after inoculation | | | |
|---|---|---|---|---|---|
| | | $5^{th}$ | $7^{th}$ | $9^{th}$ | $12^{th}$ |
| **3** | 50 | 0.26 ± 0.21[a,b] (64.4) | 1.63 ± 0.91 (24.5) | 1.23 ± 0.26 (38.2) | 9.7 ± 4.42 (8.69) |
| | 20 | 0.53 ± 0.25 (26.5) | 1.4 ± 0.31(35.3) | 2.34 ± 0.90 (0) | 12.25 ± 6.42 (0) |
| | 10 | 0.59 ± 0.49 (19.2) | 1.5 ± 0.62 (30.4) | 3.07 ± 1.7 (0) | 15.95 ± 7.86 (0) |
| AS/MQ | 5/10 | 0.06 ± 0.03[a] (91.3) | 0.10 ± 0.05[a](95.3) | 0.18 ± 0.10[a] (90.9) | 0.77 ± 0.72[a] (92.7) |
| Water | - | 0.73 ± 0.29 | 2.16 ± 1.08 | 1.99 ± 0.76 | 10.62 ± 7.24 |

AS= Artesunate MQ=Mefloquine SD=Standard Deviation

[a] = p-value < 0.05 (compared to water-treated group)
[b] = p-value > 0.05 (compared to AS/MQ-treated group)

The parasitemia of infected mice treated with 50 mg/kg of compound **3** was statistically different from water-treated group (Mann-Whitney test, p-value <0.05). Therefore, no statistical difference was observed comparing the treatment with compound **3** (50 mg/kg) and standard antimalarials on day 5 (Mann-Whitney test, p-value >0.05).

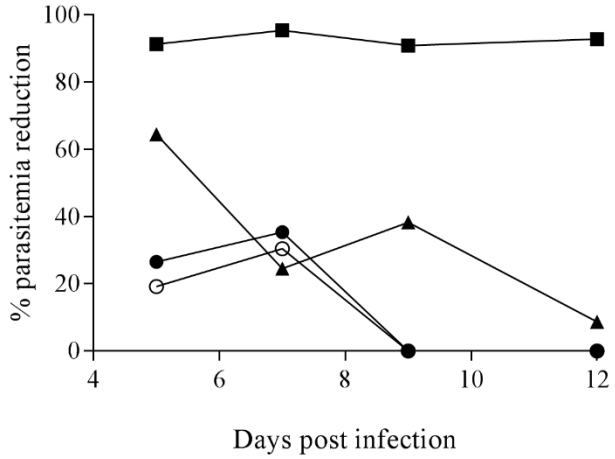


**Figure 7.** Percentage of parasitemia reduction at days 5, 7, 9 and 12 after the beginning of the treatment. Compound **3** 50mg/kg/day(▲); 20mg/kg/day (●); 10mg/kg/day(○) and AS 5mg/kg/day + MQ 10mg/kg/day (■).

The overall mortality in all infected groups is shown in Figure 8. No statistical difference was found between treatments. Therefore, at the end of the experiment, 80 % of the mice survived on the group treated with 50 mg/kg of compound **3**, as well as the AS/MQ group. Moreover, no weight loss was observed on treated mice, indicating that the gavage did not wound the stomachs of the mice. The group treated with artesunate and mefloquine did gain weight, probably due to the fast recovering from the infection (data not shown).

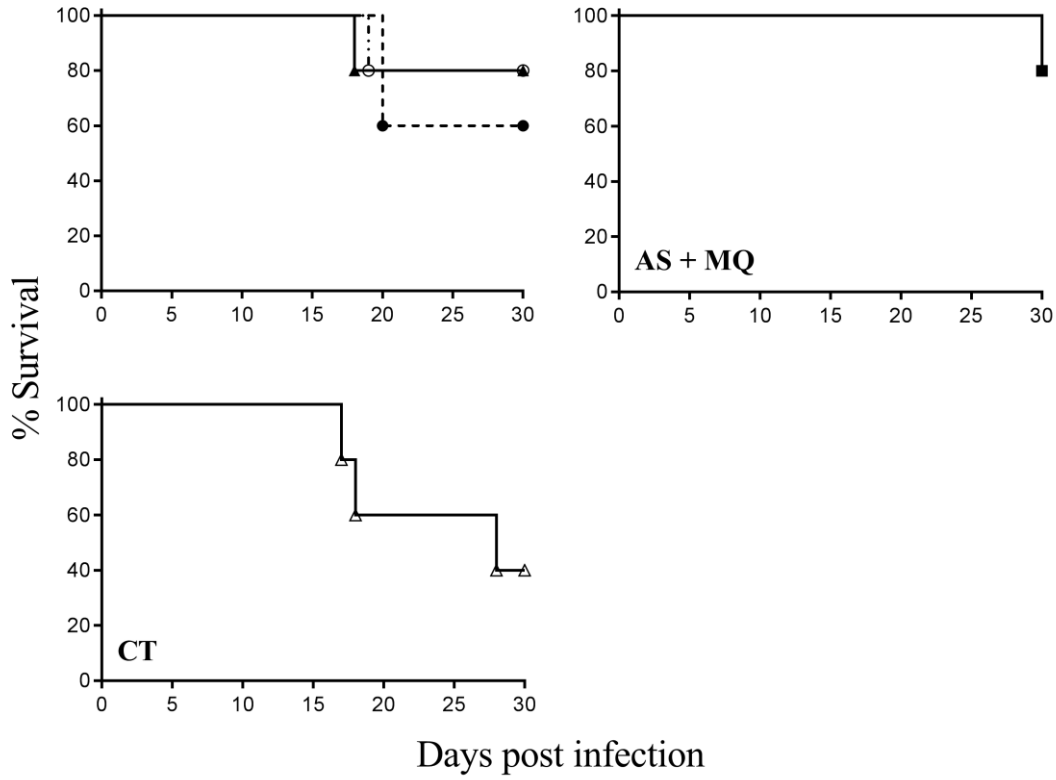


**Figure 8.** Survival of *P. berghei* infected mice after 4-day oral treatment. Mice survival were evaluated for 30 days. Compound **3**, 50mg/kg/day (▲);20mg/kg/day (●);10mg/kg/day (○); AS/MQ, 5mg/kg/day of AS + 10mg/kg/day of MQ (■), and non-treated controls (CT) (Δ).

Drug discovery projects, like Medicines for Malaria Venture (MMV) or Drugs for Neglected Diseases initiative (DNDi), established that a new clinical candidate molecule should have a high *in vivo* efficacy ($10^6$-fold parasite reduction) with an oral and single dose (Burrows et al., 2013). Despite compound **3** did not exhibit this pattern of action, it is important to mention that the *in vivo* tests were carried out with a model of rodent malaria, instead a *Plasmodium falciparum*-infected severe combined immunodeficient (SCID) mouse model. SCID is considered the gold pattern to establish antimalarial *in vivo* results (Kaushansky et al., 2014). Although, parasite clearance is not the only criteria adopted in the checkpoint for the development of a new antimalarial. Other parameters like: i) easy of synthesis with low cost, ii) good oral bioavailability,

iii) drug metabolism, and iv) good membrane permeability are properties that can lead to success in final phases of clinical trials (Gayvert et al., 2016).

In this context, in order to determine the membrane permeability of compound **3**, we performed Caco-2 permeability assay.

### 3.8. *Compound 3 uptake by Caco-2 cell line*

Both compound **3** and CQ were evaluated for their Caco-2 cell line uptake. The uptake of compound **3** increased linearly according to the incubation time and after 60 min no statistical difference was observed when compared to CQ (Figure 9). These results suggest that compound **3** is a good candidate for oral administration.

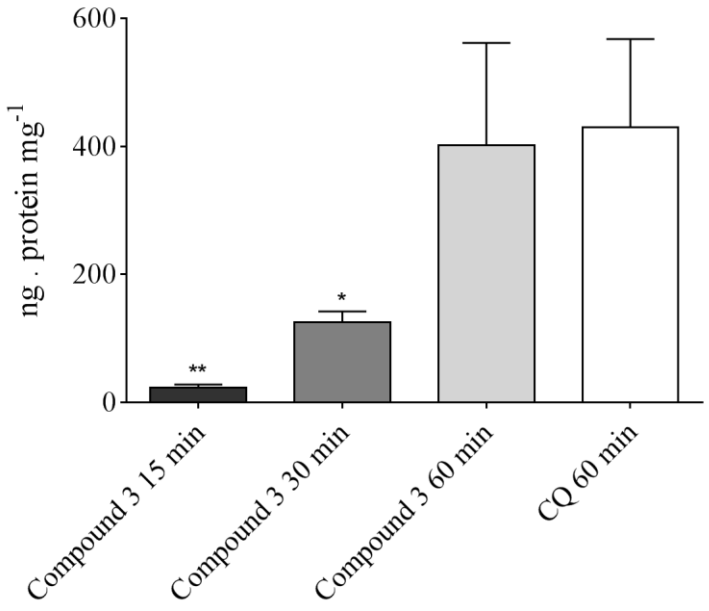


**Figure 9**. Uptake of compound **3** (100 µM) and chloroquine (100 µM) by Caco-2 cells (n=3) after incubation at 37 °C in Hank´s balanced salt solution pH 7.4. * $p < 0.05$, ** $p<0.01$ when compared to the CQ. Mean ± SD. CQ – Chloroquine

The permeability and uptake characteristics of CQ in Caco-2 cell model was systematically investigated (Augustijns, 1996). After 60 min of incubation in the presence of CQ (100 µM), the uptake was about 24 µg per mg of protein. This result is

about 30-fold higher than that found in our study. Such discrepancies can be attributed to the differences in culture conditions and cell density (Bentz et al., 2013).

## 4. Conclusions

In conclusion, we optimized the development of a previously reported 3-APA hit compound to a new thiazole lead. Compound **3** has a potent antimalarial activity with a great selectivity index. This compound is not mutagenic and is capable of inhibiting *P. berghei in vivo* development. We also determined that the uptake of compound **3** by Caco-2 cells is similar to CQ and it acts within the parasite's food vacuole, as predicted by *in silico* and UV-vis studies. Thus, compound **3** presents a promising lead for optimization as an antimalarial new drug with high selectivity, low toxicity, good membrane permeability. Ongoing studies are focused on to establish the in vivo PK/PD profile of compound **3.**

## Acknowledgments

This work was supported by the Brazilian Agencies: CNPq, FAPEMIG, FAPESP and CAPES. We thank the Multiuser Multiphoton Confocal Microscopy Laboratory (INFAR-UNIFESP) for the access to confocal microscopy devices. The authors also thank the Cellular Biology Service from the Ezequiel Dias Foundation for donation of the human cell lines.

## References

Andrade-Neto, V.F., Brandão, M.G.L., Stehmann, J.R., Oliveira, L. a., Krettli, A.U., 2003. Antimalarial activity of Cinchona-like plants used to treat fever and malaria in Brazil. J. Ethnopharmacol. 87, 253–256. https://doi.org/10.1016/S0378-

8741(03)00141-7

Ashley, E.A., Phyo, A.P., 2018. Drugs in Development for Malaria. Drugs 78, 861–879. https://doi.org/10.1007/s40265-018-0911-9

Augustijns, P.F., 1996. Uptake and Transport Characteristics of Chloroquine in an In-vitro Cell Culture System of the Intestinal Mucosa, Caco-2. J. Pharm. Pharmacol. 48, 277–280. https://doi.org/10.1111/j.2042-7158.1996.tb05916.x

Baker, D.A., Stewart, L.B., Large, J.M., Bowyer, P.W., Ansell, K.H., Jiménez-Díaz, M.B., El Bakkouri, M., Birchall, K., Dechering, K.J., Bouloc, N.S., Coombs, P.J., Whalley, D., Harding, D.J., Smiljanic-Hurley, E., Wheldon, M.C., Walker, E.M., Dessens, J.T., Lafuente, M.J., Sanz, L.M., Gamo, F.-J., Ferrer, S.B., Hui, R., Bousema, T., Angulo-Barturén, I., Merritt, A.T., Croft, S.L., Gutteridge, W.E., Kettleborough, C.A., Osborne, S.A., 2017. A potent series targeting the malarial cGMP-dependent protein kinase clears infection and blocks transmission. Nat. Commun. 8, 430. https://doi.org/10.1038/s41467-017-00572-x

Barbosa, C. de S., Guimarães, D.S.M., Gonçalves, A.M.M.N., Barbosa, M.C. da S., Alves e Costa, M.L., Nascimento Júnior, C.S., Guimarães, L., Ribeiro-Viana, R.M., dos Santos, F.V., Alves de Brito, C.F., de Pilla Varotti, F., Ribeiro Viana, G.H., 2017. Target-Guided Synthesis and Antiplasmodial Evaluation of a New Fluorinated 3-Alkylpyridine Marine Alkaloid Analog. ACS Omega 2, 8264–8272. https://doi.org/10.1021/acsomega.7b01302

Barbosa, M.C.S., de Souza Barbosa, C., de Oliveira, J.T., Moreira, N.C.S., de Miranda Martins, N.R., Alves Gomes, G.K., Caldeira, C.A., Alves e Costa, M.L., Martins Guimarães, D.S., Guimarães, L., Nascimento, C.S., de Pilla Varotti, F., Ribeiro Viana, G.H., Santos, F.V. dos, 2018. Synthesis and evaluation of the mutagenicity

of 3-alkylpyridine marine alkaloid analogues with anticancer potential. Mutat. Res. Toxicol. Environ. Mutagen. 825, 31–39. https://doi.org/10.1016/j.mrgentox.2017.11.006

Bennett, T.N., Kosar, A.D., Ursos, L.M.B., Dzekunov, S., Singh Sidhu, A.B., Fidock, D.A., Roepe, P.D., 2004. Drug resistance-associated pfCRT mutations confer decreased Plasmodium falciparum digestive vacuolar pH. Mol. Biochem. Parasitol. 133, 99–114.

Bentz, J., O'Connor, M.P., Bednarczyk, D., Coleman, J., Lee, C., Palm, J., Pak, Y.A., Perloff, E.S., Reyner, E., Balimane, P., Brannstrom, M., Chu, X., Funk, C., Guo, A., Hanna, I., Heredi-Szabo, K., Hillgren, K., Li, L., Hollnack-Pusch, E., Jamei, M., Lin, X., Mason, A.K., Neuhoff, S., Patel, A., Podila, L., Plise, E., Rajaraman, G., Salphati, L., Sands, E., Taub, M.E., Taur, J.-S., Weitz, D., Wortelboer, H.M., Xia, C.Q., Xiao, G., Yabut, J., Yamagata, T., Zhang, L., Ellens, H., 2013. Variability in P-Glycoprotein Inhibitory Potency (IC50) Using Various in Vitro Experimental Systems: Implications for Universal Digoxin Drug-Drug Interaction Risk Assessment Decision Criteria. Drug Metab. Dispos. 41, 1347–1366. https://doi.org/10.1124/dmd.112.050500

Bradford, M.M., 1976. A rapid and sensitive method for the quantitation of microgram quantities of protein utilizing the principle of protein-dye binding. Anal. Biochem. 72, 248–254. https://doi.org/10.1016/0003-2697(76)90527-3

Burrows, J.N., Duparc, S., Gutteridge, W.E., Hooft van Huijsduijnen, R., Kaszubska, W., Macintyre, F., Mazzuri, S., Möhrle, J.J., Wells, T.N.C., 2017. New developments in anti-malarial target candidate and product profiles. Malar. J. 16, 26. https://doi.org/10.1186/s12936-016-1675-x

Burrows, J.N., van Huijsduijnen, R.H., Möhrle, J.J., Oeuvray, C., Wells, T.N.C., Hooft van Huijsduijnen, R., Möhrle, J.J., Oeuvray, C., Wells, T.N.C., van Huijsduijnen, R.H., Möhrle, J.J., Oeuvray, C., Wells, T.N.C., 2013. Designing the next generation of medicines for malaria control and eradication. Malar. J. 12, 187. https://doi.org/10.1186/1475-2875-12-187

Carmichael, J., DeGraff, W.G., Gazdar, A.F., Minna, J.D., Mitchell, J.B., 1987. Evaluation of a tetrazolium-based semiautomated colorimetric assay: assessment of chemosensitivity testing. Cancer Res. 47, 936–42.

Collins, A.R., 2004. The Comet Assay for DNA Damage and Repair: Principles, Applications, and Limitations. Mol. Biotechnol. 26, 249–261. https://doi.org/10.1385/MB:26:3:249

de Oliveira, J.T., Barbosa, M.C. da S., de Camargos, L.F., da Silva, I.V.G., Varotti, F. de P., da Silva, L.M., Moreira, L.M., Lyon, J.P., dos Santos, V.J. da S.V., dos Santos, F.V., 2017. Digoxin reduces the mutagenic effects of Mitomycin C in human and rodent cell lines. Cytotechnology 69, 699–710. https://doi.org/10.1007/s10616-017-0078-3

Eastmond, D.A., Tucker, J.D., 1989. Identification of aneuploidy-inducing agents using cytokinesis-blocked human lymphocytes and an antikinetochore antibody. Environ. Mol. Mutagen. 13, 34–43. https://doi.org/10.1002/em.2850130104

Egan, T.J., 2008. Haemozoin formation. Mol. Biochem. Parasitol. 157, 127–136. https://doi.org/10.1016/j.molbiopara.2007.11.005

El Chamy Maluf, S., Dal Mas, C., Oliveira, E.B., Melo, P.M., Carmona, A.K., Gazarini, M.L., Hayashi, M.A.F., 2016. Inhibition of malaria parasite Plasmodium

falciparum development by crotamine, a cell penetrating peptide from the snake venom. Peptides 78, 11–16. https://doi.org/10.1016/j.peptides.2016.01.013

Fenech, M., 2007. Cytokinesis-Block Micronucleus Cytome Assay, in: Nature Protocols. pp. 1084–1104. https://doi.org/10.1007/978-1-60327-409-8_16

Ferrao, J., Niquisse, S., Mendes, J., Painho, M., 2018. Mapping and Modelling Malaria Risk Areas Using Climate, Socio-Demographic and Clinical Variables in Chimoio, Mozambique. Int. J. Environ. Res. Public Health 15, 795. https://doi.org/10.3390/ijerph15040795

Gayvert, K.M., Madhukar, N.S., Elemento, O., 2016. A Data-Driven Approach to Predicting Successes and Failures of Clinical Trials. Cell Chem. Biol. 23, 1294–1301. https://doi.org/10.1016/j.chembiol.2016.07.023

Gomes, C.C., Moreira, L.M., Santos, V.J.S.V.S. V, Ramos, A.S., Lyon, J.P., Soares, C.P., Santos, F. V., Bosco, C.D., João, S., Rei, D., 2011. Assessment of the genetic risks of a metallic alloy used in medical implants. Genet. Mol. Biol. 34, 116–21. https://doi.org/10.1590/S1415-47572010005000118

Gonçalves, A.M.M.N., de Lima, A.B., da Silva Barbosa, M.C., de Camargos, L.F., de Oliveira, J.T., de Souza Barbosa, C., Villar, J.A.F.P., Costa, A.C., Silva, I.V.G. Da, Silva, L.M., de Pilla Varotti, F., Dos Santos, F.V., Viana, G.H.R., 2014. Synthesis and biological evaluation of novel 3-alkylpyridine marine alkaloid analogs with promising anticancer activity. Mar. Drugs 12, 4361–78. https://doi.org/10.3390/md12084361

Hibbert, D. B., Thordarson, P., 2016. The death of the Job plot, transparency, open science and online tools, uncertainty estimation methods and other developments

in supramolecular chemistry data analysis. Chem. Commun. 52, 12792-12805. https://doi.org/10.1039/C6CC03888C

Hilário, F.F., de Paula, R.C., Silveira, M.L.T., Viana, G.H.R., Alves, R.B., Pereira, J.R.C.S., Silva, L.M., de Freitas, R.P., de Pilla Varotti, F., 2011. Synthesis and evaluation of antimalarial activity of oxygenated 3-alkylpyridine marine alkaloid analogues. Chem. Biol. Drug Des. 78, 477–82. https://doi.org/10.1111/j.1747-0285.2011.01154.x

Ji, Z., Ball, N.S., LeBaron, M.J., 2017. Global regulatory requirements for mutagenicity assessment in the registration of industrial chemicals. Environ. Mol. Mutagen. 58, 345–353. https://doi.org/10.1002/em.22096

Kalaria, P.N., Karad, S.C., Raval, D.K., 2018. A review on diverse heterocyclic compounds as the privileged scaffolds in antimalarial drug discovery. Eur. J. Med. Chem. 158, 917–936. https://doi.org/10.1016/j.ejmech.2018.08.040

Katsuno, K., Burrows, J.N., Duncan, K., van Huijsduijnen, R.H., Kaneko, T., Kita, K., Mowbray, C.E., Schmatz, D., Warner, P., Slingsby, B.T., 2015. Hit and lead criteria in drug discovery for infectious diseases of the developing world. Nat. Rev. Drug Discov. 14, 751–758. https://doi.org/10.1038/nrd4683

Kaushansky, A., Mikolajczak, S.A., Vignali, M., Kappe, S.H.I., 2014. Of men in mice: the success and promise of humanized mouse models for human malaria parasite infections. Cell. Microbiol. 16, 602–611. https://doi.org/10.1111/cmi.12277

Kirsch-Volders, M., Bonassi, S., Knasmueller, S., Holland, N., Bolognesi, C., Fenech, M.F., 2014. Commentary: Critical questions, misconceptions and a road map for improving the use of the lymphocyte cytokinesis-block micronucleus assay for in

vivo biomonitoring of human exposure to genotoxic chemicals-A HUMN project perspective. Mutat. Res. - Rev. Mutat. Res. 759, 49–58. https://doi.org/10.1016/j.mrrev.2013.12.001

Kumawat, M.K., 2017. Thiazole Containing Heterocycles With Antimalarial Activity. Curr. Drug Discov. Technol. 14, 1–5. https://doi.org/10.2174/1570163814666170725114159

Lambros, C., Vanderberg, J.P., 1979. Synchronization of plasmodium-falciparum erythrocytic stages in culture. J. Parasitol. 65, 418–420. https://doi.org/10.2307/3280287

Lobo, L., Cabral, L.I.L., Sena, M.I., Guerreiro, B., Rodrigues, A.S., De Andrade-Neto, V.F., Cristiano, M.L.S., Nogueira, F., 2018. New endoperoxides highly active in vivo and in vitro against artemisinin-resistant Plasmodium falciparum. Malar. J. 17, 1–11. https://doi.org/10.1186/s12936-018-2281-x

Lodha, B., Bhadane, R., Patel, B., Killedar, D., 2008. Biodegradation of pyridine by an isolated bacterial consortium/strain and bio-augmentation of strain into activated sludge to enhance pyridine biodegradation. Biodegradation 19, 717–723. https://doi.org/10.1007/s10532-008-9176-4

Martin, R.E., Shafik, S.H., Richards, S.N., 2018. Mechanisms of resistance to the partner drugs of artemisinin in the malaria parasite. Curr. Opin. Pharmacol. 42, 71–80. https://doi.org/10.1016/j.coph.2018.07.010

Mishra, M., Mishra, V.K., Kashaw, V., Iyer, A.K., Kashaw, S.K., 2017. Comprehensive review on various strategies for antimalarial drug discovery. Eur. J. Med. Chem. 125, 1300–1320. https://doi.org/10.1016/j.ejmech.2016.11.025

Mudliar, S.N., Padoley, K.V., Bhatt, P., Sureshkumar, M., Lokhande, S.K., Pandey, R.A., Vaidya, A.N., 2008. Pyridine biodegradation in a novel rotating rope bioreactor. Bioresour. Technol. 99, 1044–1051. https://doi.org/10.1016/j.biortech.2007.02.039

Noedl, H., Wernsdorfer, W.H., Miller, R.S., Wongsrichanalai, C., 2002. Histidine-rich protein II: a novel approach to malaria drug sensitivity testing. Antimicrob. Agents Chemother. 46, 1658–64. https://doi.org/10.1128/AAC.46.6.1658

Nsanzabana, C., 2019. Resistance to Artemisinin Combination Therapies (ACTs): Do Not Forget the Partner Drug! Trop. Med. Infect. Dis. 4, 26. https://doi.org/10.3390/tropicalmed4010026

Olive, P.L., Banáth, J.P., 2006. The comet assay: a method to measure DNA damage in individual cells. Nat. Protoc. 1, 23–9. https://doi.org/10.1038/nprot.2006.5

Padoley, K.V., Rajvaidya, A.S., Subbarao, T.V., Pandey, R.A., 2006. Biodegradation of pyridine in a completely mixed activated sludge process. Bioresour. Technol. 97, 1225–1236. https://doi.org/10.1016/j.biortech.2005.05.020

Penzo, M., de las Heras-Dueña, L., Mata-Cantero, L., Diaz-Hernandez, B., Vazquez-Muñiz, M.-J., Ghidelli-Disse, S., Drewes, G., Fernandez-Alvaro, E., Baker, D.A., 2019. High-throughput screening of the Plasmodium falciparum cGMP-dependent protein kinase identified a thiazole scaffold which kills erythrocytic and sexual stage parasites. Sci. Rep. 9, 7005. https://doi.org/10.1038/s41598-019-42801-x

Peters, W., 1965. Drug resistance in Plasmodium berghei Vincke and Lips, 1948. I. Chloroquine resistance. Exp. Parasitol. 17, 80–9.

Ribeiro-Viana, R.M., Butera, A.P., Santos, E.S., Tischer, C.A., Alves, R.B., Pereira de

Freitas, R., Guimarães, L., Varotti, F.P., Viana, G.H.R., Nascimento, C.S., 2016. Revealing the Binding Process of New 3-Alkylpyridine Marine Alkaloid Analogue Antimalarials and the Heme Group: An Experimental and Theoretical Investigation. J. Chem. Inf. Model. 56, 571–579. https://doi.org/10.1021/acs.jcim.5b00742

Sharma, D., Bansal, K.K., Sharma, A., Pathak, M., Sharma, P.C., 2019. A Brief Literature and Review of Patents on Thiazole Related Derivatives. Curr. Bioact. Compd. 15, 304–315. https://doi.org/10.2174/1573407214666180827094725

Singh, K., Kaur, H., Smith, P., de Kock, C., Chibale, K., Balzarini, J., 2014. Quinoline-pyrimidine hybrids: synthesis, antiplasmodial activity, SAR, and mode of action studies. J. Med. Chem. 57, 435–448. https://doi.org/10.1021/jm4014778

Skinner-Adams, T.S., Sumanadasa, S.D.M., Fisher, G.M., Davis, R.A., Doolan, D.L., Andrews, K.T., 2016. Defining the targets of antiparasitic compounds. Drug Discov. Today 21, 725–739. https://doi.org/10.1016/j.drudis.2016.01.002

Thakur, R.K., Joshi, P., Baranwal, P., Sharma, G., Shukla, S.K., Tripathi, R., Tripathi, R.P., 2018. Synthesis and antiplasmodial activity of glyco-conjugate hybrids of phenylhydrazono-indolinones and glycosylated 1,2,3-triazolyl-methyl-indoline-2,3-diones. Eur. J. Med. Chem. 155, 764–771. https://doi.org/10.1016/j.ejmech.2018.06.042

Thordarson, P., 2011. Determining association constants from titration experiments in supramolecular chemistry. Chem Soc Rev. 40(3):1305-23. https://doi.org/10.1039/c0cs00062k

Titenko-Holland, N., Windham, G., Kolachana, P., Reinisch, F., Parvatham, S., Osorio,

A.M., Smith, M.T., 1997. Genotoxicity of malathion in human lymphocytes assessed using the micronucleus assay in vitro and in vivo: a study of malathion-exposed workers. Mutat. Res. 388, 85–95.

Walker, E.J., Peterson, G.M., Grech, J., Paragalli, E., Thomas, J., 2018. Are we doing enough to prevent poor-quality antimalarial medicines in the developing world? BMC Public Health 18, 630. https://doi.org/10.1186/s12889-018-5521-7

World Health Organization, 2018. World Malaria Report.

Yonemitsu, K., Koreeda, A., Kibayashi, K., Ng'walali, P., Mbonde, M., Kitinya, J., Tsunenari, S., 2005. HPLC analysis of anti-malaria agent, chloroquine in blood and tissue from forensic autopsy cases in Tanzania. Leg. Med. 7, 113–116. https://doi.org/10.1016/j.legalmed.2004.10.002

Zhu, L., Lu, L., Wang, S., Wu, J., Shi, J., Yan, T., Xie, C., Li, Q., Hu, M., Liu, Z., 2017. Oral Absorption Basics, in: Developing Solid Oral Dosage Forms. Elsevier, pp. 297–329. https://doi.org/10.1016/B978-0-12-802447-8.00011-X

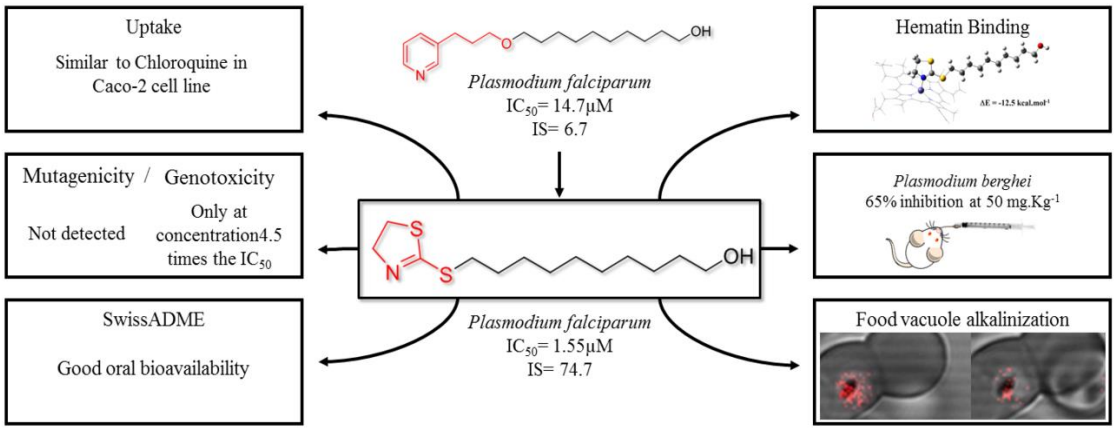


Graphical abstract